PROCEEDINGS OF SCIENCE

Results from the Muon g-2 experiment at Fermilab

Anna Driutti[a,*] **on behalf of the Muon g − 2 Collaboration**

[a] *University and INFN Pisa, Italy*

E-mail: anna.driutti@unipi.it

The goal of the Muon g-2 experiment at Fermilab is to measure the muon magnetic moment anomaly with a final accuracy of 140 parts per billion (ppb). The experiment has published two results based on the data collected in 2018 (Run-1) and 2019-2020 (Run-2/3), respectively. These results confirm the previous measurement performed 20 years ago at Brookhaven National Laboratory, and their combination reaches the unprecedented uncertainty of 200 ppb. This proceeding presents a brief overview of the Standard Model prediction for the muon g-2. It then summarizes the experimental measurement technique and the Run-1 and Run-2/3 measurements, detailing the improvements in their systematic and statistical uncertainties. Finally, it illustrates the comparison between theory and experiment and discusses future prospects.

10th International Conference on Quarks and Nuclear Physics (QNP2024)
8-12 July, 2024
Barcelona, Spain

*Speaker

PoS(QNP2024)220

1. Introduction

In the history of the Standard Model (SM) of particle physics, the magnetic moment of the muon has played a central role. It serves as a precise test of the SM and could offer potential hints of new physics. Muons are elementary particles with mass m, charge q and intrinsic angular momentum (spin) $\vec{S}$. Their magnetic momentum $\vec{\mu}$, in natural units, is expressed as:

$$\vec{\mu} = g\frac{q}{2m}\vec{S}, \tag{1}$$

where g is the so called gyromagnetic ratio or g-factor. In 1928, Dirac, in his "Quantum Theory of the Electron", predicted $g = 2$ for the electrons [1], and consequently for all spin-$\frac{1}{2}$ particles, including muons. Relativistic quantum electrodynamics predicts that g is slightly higher than 2 due to interactions with virtual particles. These additional radiative correction affect g by a value described by the muon magnetic anomaly, defined as:

$$a_\mu = \frac{g-2}{2}. \tag{2}$$

In the framework of the SM, all particles and interactions described by the Quantum ElectroDynamics (QED), ElectroWeak (EW), and Quantum ChromoDynamics (QCD) theories are involved in calculating a_μ. Consequently, if new particles not included in the SM contribute, the experimental value of a_μ will differ from the theoretical prediction. For the past two decades, a discrepancy of about 3.7 standard deviations (sigmas, σ) has persisted between the experimental value of the muon anomaly (published in 2006 by the Muon g-2 Brookhaven National Laboratory, BNL, Collaboration) and the theoretical evaluations [2]. This discrepancy has motivated both the experimentalists and theorists to pursue more precise measurements and calculations of a_μ. The following sections will first summarize the current status of the theoretical SM calculation of a_μ and then review in detail the latest experimental measurements performed at Fermilab.

2. The Standard Model calculation of a_μ

The SM theoretical calculation is determined by summing the following terms:

$$a_\mu^{\mathrm{SM}} = a_\mu^{\mathrm{QED}} + a_\mu^{\mathrm{EW}} + a_\mu^{\mathrm{HVP}} + a_\mu^{\mathrm{HLbL}}, \tag{3}$$

namely, the Quantum ElectroDynamics (QED), ElectroWeak (EW), the Hadronic Vacuum Polarization (HVP), and the Hadronic Light-by-Light (HLbL) contributions. The QED term, a_μ^{QED}, is the larger contributor but has the smallest uncertainty (1 ppb). The EW term, a_μ^{EW}, also has a small uncertainty (10 ppb), in fact the total uncertainty, $\delta a_\mu^{\mathrm{SM}}$ is dominated by the hadronic contributions (the HVP and the HLbL terms). Table 1 reports the contribution and the uncertainty of each term, along with the total theoretical calculation of a_μ.

2.1 The Quantum ElectroDynamics contribution

The QED term, a_μ^{QED}, comprises all contributions from photons and leptons interactions. It includes a lepton-mass independent part, which dominates the contribution, and a lepton-mass dependent part, which depends on the ratio between lepton masses. This QED term has been

Contribution		Value ($\times 10^{-11}$)	Ref.
a_μ^{QED}		116 584 718.931 (104)	[3]
a_μ^{EW}		153.6 (1.0)	[3]
	(LO, e^+e^- WP)	6931 (40)	[3]
a_μ^{HVP}	(LO, lattice-QCD BMW)	7075 (55)	[4]
	(NLO + NNLO, e^+e^- WP)	-98.3 (7) + 12.4 (1)	[3]
a_μ^{HLbL}	(phenomenology + lattice + NLO)	92 (18)	[3]
a_μ^{SM}		116 591 810 (43) 116 591 954 (57)	[3] [4]

Table 1: Value of a_μ^{SM} with all terms detailed. The HVP term is divided into leading-order (LO) and next-to-LO plus next-to-next-to-LO (NLO + NNLO) parts. For the LO two predictions are reported: one obtained with a data-driven dispersive approach (using $e^+e^- \to$ hadrons experimental data, to which we refer as WP evaluation since it is the consensus prediction obtained in the White Paper Ref. [3]), and one performed with lattice-QCD calculations (to which we refer as BMW evaluation). See Section 2.3 for additional details.

calculated [3] using the perturbation theory, involving the summation of 12,672 Feyman diagrams, up to five-loop order. The uncertainty in this term, $\delta a_\mu^{\mathrm{QED}}$, is primarily due to the uncertainties in the four-, five- and estimated six-loop QED contributions, the τ-lepton mass and α, the fine-structure constant.

2.2 The ElectroWeak contribution

The EW term, a_μ^{EW}, involves the summation of the Feyman diagrams that contain the exchange of electroweak gauge bosons: the W and Z bosons, and the Higgs boson. It has been calculated [3] by summing numerical results of the one-loop diagrams, the bosonic and four fermionic two-loop diagrams and the leading three-loop logarithms contributions. These contributions are suppressed by the large masses of the involved gauge bosons, hence the EW term is much smaller than the QED and HVP terms, but comparable in order of magnitude to the HLbL term. The uncertainty of a_μ^{EW} is ten times larger than $\delta a_\mu^{\mathrm{QED}}$, but negligible with respect to the uncertainties of a_μ^{HVP} and a_μ^{HLbL} terms, and it is dominated by the uncertainty of the calculation involving two-loop Feynman diagrams that contain heavy particles and a photon, specifically those that need significant non-perturbative corrections.

2.3 The Hadronic contributions

The hadronic contributions, a_μ^{HVP} and a_μ^{HLbL} cannot be calculated using the perturbation theory at low energies due to the non-perturbative nature of the QCD, and thus are calculated mainly employing two methods: data-driven approaches (using the dispersive relations) or from lattice-QCD. For the HLbL term the two methods yield compatible results with an uncertainty that amounts to 150 ppb of a_μ^{SM}, while the current calculations of the HVP term are showing significant tensions.

2.3.1 The Hadronic Vacuum Polarization contribution

The HVP term, a_μ^{HVP}, contains the contributions of the Feyman diagrams that involve strongly interacting particles. In the data-driven approaches, by utilizing the principles of unitarity and

analyticity, these loop integrals can be expressed as dispersion integrals. The leading-order hadronic vacuum polarization (LO-HVP) with this dispersion relation approach is evaluated using [3]:

$$a_\mu^{\text{LO-HVP}} = \frac{\alpha^2}{3\pi^2} \int_{M_{\pi^0}^2}^{\infty} \frac{K(s)}{s} R(s)\, ds, \tag{4}$$

where M_{π^0} is the mass of the neutral pion, $K(s)$ is the QED kernel function and $R(s)$ is the ratio between the $e^+e^- \rightarrow hadrons$ bare cross section and the $e^+e^- \rightarrow \mu^+\mu^-$ one evaluated at the center-of-mass energy $\sqrt{s}$. This $R(s)$ ratio is determined using a compilation of hadronic cross-section experimental data as inputs. All decay channels are considered, and the measurements are collected from different e^+e^- experiments. The channel that contributes the most is $e^+e^- \rightarrow \pi^+\pi^-$. Currently, discrepancies at the level of $2.5 - 5\,\sigma$ exist among cross-section measurements from different experiments [5]. In particular, a new result published by the CMD-3 experiment at Novosibirsk [6], released after the a_μ^{HVP} (LO, e^+e^- WP) of table 1, differs significantly from the previous measurements.

A complementary approach to compute the LO-HVP is from lattice-QCD calculations. These calculations are performed in the Euclidean space and involve weighted integrals of correlation functions over Euclidean time. The a_μ^{HVP} (LO, lattice-QCD) term is obtained by summing over all quark-flavors and includes both connected and disconnected contractions [7]. In April 2021, the BMW collaboration published the a_μ^{HVP} (LO, lattice-QCD BMW) reported in table 1. This result is the first complete lattice-QCD result with a precision comparable with the data-driven evaluation, and it is 2.1σ higher than a_μ^{HVP} (LO, e^+e^- WP).

The higher order contributions, *i.e.*, next-to-leading order (NLO) and next-next-to-leading order (NNLO) contributions, are evaluated using dispersion integral similar to equation 4.

2.3.2 The Hadronic Light-by-Light contribution

The HLbL scattering term, a_μ^{HLbL}, can be pictured as a sum of diagrams with single-meson exchange and diagrams with hadron loops at low energies, but at high energies, it can be described by perturbative quark loops [3]. Its magnitude is two orders smaller than the HVP term, as it is $O(\alpha^3)$. This term is calculated in a similar way to the HVP term, using either data-driven dispersive approach or from lattice-QCD calculations. The results from these two calculation methods are found to be in good agreement with each other [5].

3. The experimental measurements of a_μ

The Muon g-2 experiment at Fermilab began collecting data in 2018, aiming to measure $a_\mu^{\text{Exp.}}$ with an unprecedented precision of 140 ppb, comprising 100 ppb systematic uncertainty and 100 ppb statistical uncertainty [8]. To obtain this precision, operations continued until summer 2023, resulting in a total statistic of approximately 334.5 billion of positrons from muon decay. This is about 21 times the statistics collected by the previous BNL experiment, E821, which completed data taking in 2001. These data are divided into 6 datasets (Run-1 to Run-6), with a final expected statistical uncertainty of 100 ppb.

3.1 Methodology

The muons were produced by the Fermilab Accelerator Complex [8, 9] by colliding protons on a target. The protons were first accelerated in the LINAC and booster synchrotron to kinetic energy of 8 GeV, and they were then divided into 4 bunches in the recycler synchrotron. Each bunch collided with an Inconel target at the target station, producing a secondary beam of pions. This pion beam was then sent to the delivery ring through a 280 m transfer line, where the pions decayed into muons. Only polarized muons with 3.1 GeV/c momentum were selected and then separated from proton and pions as they traveled around the delivery ring. Finally, this polarized positive muon beam was sent to the Muon Campus building MC1, ready for being injected into the storage ring of the Muon g-2 experiment.

The muon storage ring, used to store the muons and to provide the required 1.45 T magnetic field ($\vec{B}$) for the a_μ measurement, was the same one used by the BNL Experiment. The ring, made of three superconducting coils and a continuous "C-shaped" yoke to allow the positrons from the decay of the muons to reach the detectors, was disassembled at BNL and relocated at Fermilab in the summer of 2013 [8]. Although the coils and yoke were reused from the previous experiment, many improvements were made to achieved a magnetic field uniformity of 14 ppm RMS (three times better than at BNL): passive elements, such as low-carbon steel poles, edge shims and wedges, as well as active elements, such as surface correction coils, were meticulously placed and adjusted around the storage region [10]. The storage ring was also instrumented with two in-vacuum straw tracker stations and 24 electromagnetic calorimeters placed on the inner circumference [11].

The muons entered the storage ring through a hole in the iron yoke where an inflector magnet was placed to provide a nearly magnetic-field-free region. Before the injection, the T0-counter, a thin scintillator read out by photomultiplier tubes, measured the time profile of the beam. The spatial profile of the beam, before and after the injection, was measured by the inflector beam monitoring system (IBMS). The injected polarized muons were then deflected by approximately 10 mrad onto the center of the storage region by three fast pulsed magnets called kicker magnets. The muons were then left to circulate around the ring for 1 ms (a fill), vertically focused by a set of four electrostatic quadrupoles (ESQs). Their motion is characterized by a cyclotron frequency $\vec{\omega}_C$, and a spin precession frequency $\vec{\omega}_S$ with the difference between these two observables, called muon anomalous precession frequency ($\vec{\omega}_a$), being at first order proportional to the anomalous magnetic moment of the muon:

$$\vec{\omega}_a = -\frac{q}{m}\left[a_\mu \vec{B} - \left(a_\mu - \frac{1}{\gamma^2-1}\right)\frac{\vec{\beta}\times\vec{E}}{c} - a_\mu\left(\frac{\gamma}{\gamma+1}\right)(\vec{\beta}\cdot\vec{B})\vec{\beta}\right] \simeq -\frac{q}{m}a_\mu\vec{B}. \tag{5}$$

In equation 6, q and m represent the mass and electric charge of the muon respectively, $\vec{\beta}$ the muon velocity with respect of speed of light c, and γ the muon's Lorenz factor. The rightmost expression is valid since, at first order, the second and third terms in the square bracket vanish. The second term, proportional to the ESQ's electric field $\vec{E}$, vanishes for $\gamma = \sqrt{(1+1/a_\mu)} \approx 29.3$ which correspond to the so-called magic momentum, $p_0 \approx 3.094$ GeV/c, at which the muons are injected. The third term, proportional to $(\vec{\beta}\cdot\vec{B})$, cancels out because the muons travel mostly orthogonally to the magnetic field. The muon anomaly is then determined [13] by multiplying the

ratio of frequencies $\mathcal{R}'_\mu(T_r) = \omega_a/\widetilde{\omega}'_p(T_r)$, which is directly measured by the experiment, with a factor $\mathcal{F}_{ext}$, which is a set of well known fundamental factors taken from literature [12]:

$$a_\mu = \frac{\omega_a}{\widetilde{\omega}'_p(T_r)}\,\mathcal{F}_{ext}. \tag{6}$$

The denominator of $\mathcal{R}'_\mu(T_r)$, $\widetilde{\omega}'_p(T_r)$, represents the magnetic field magnitude, B, in terms of shielded (*i.e.*, measured in spherical water sample at $T_r = 34.7°$C) proton precession frequency, weighted by the muon distribution. It is measured [10] by mapping the storage volume using 17 nuclear magnetic resonance (NMR) probes, calibrated with a pure-water sample, placed in a trolley. This mapping occurred every few days when the beam is stopped. The resulting B-field maps are then interpolated with the field measured continuously by 378 fixed NMR probes that were located above and below the storage region around the azimuth. The maps are then weighted by the temporal and spatial distributions of the muons, which are extrapolated from the positron trajectory measured by the tracker and simulations. Finally, two corrections are applied to account for the magnetic transient fields: one due to the eddy currents produced by kicker pulses (kickers transient field correction, B_k) and the other due to the mechanicals vibration from pulsing the ESQs (quadrupoles transient field correction, B_q). The B_k correction was measured using Faraday magnetometers, while the B_q correction was mapped using special NMR probes.

The numerator of $\mathcal{R}'_\mu(T_r)$, the anomalous precession frequency ω_a, represents the muon spin evolution with respect to its momentum during a fill. It is measured [11] by fitting the rate of positrons, $N(t)$, recorded by the calorimeter system during the fill (the so-called wiggle plot). In fact, due to parity violation in the weak decay $\mu^+ \rightarrow e^+\nu_e\bar{\nu}_\mu$, high-energy positrons carry the information on the average muon spin direction, and $N(t) \propto \left[1 + A\cos(\omega_a^m t + \varphi)\right]$, where A and φ are the g-2 asymmetry and phase, respectively. Corrections are then applied to the fitted ω_a^m to account for residual beam dynamics effects [14]. Two corrections, the electric field and pitch corrections, are applied to account for the second-order effects of the second and third terms in the square bracket of equation 6. Additionally, three corrections - the muon losses, differential decay and phase acceptance - are applied to account for fill-time-dependent phase-changing effects.

3.2 Results

The measurement is also blinded by applying a blinding factor to the digitization rate of the experiment clock system. This factor is revealed only when the physics analysis of an entire Run is completed. At present, the Run-1 result [15] and the Run-2/3 results [16] have been unblinded and published in 2021 and 2023, respectively. Results from Run-4/5/6 are expected to be release in 2025. The Run-1 and Run-2/3 results are in agreement with each other, and when combined, they reach an uncertainty of 203 ppb. Both Run-1 and Run-2/3 uncertainties are still statistical dominated, but the Run-2/3 result has a systematic uncertainty of 70 ppb which is lower than the 100 ppb design goal of the Fermilab Muon g-2 experiment. These results confirmed the previous measurement published in 2006 by the BNL collaboration.

Figure 1 and Table 2 report the Fermilab Run-1 ($a_\mu^{\text{FNAL, Run}-1}$) and Run-2/3 ($a_\mu^{\text{FNAL, Run}-2/3}$) results, their combination ($a_\mu^{\text{FNAL, Run}-1/2/3}$), the previous result from BNL (a_μ^{BNL}) and the experimental world average ($a_\mu^{\text{Exp. Average}}$).

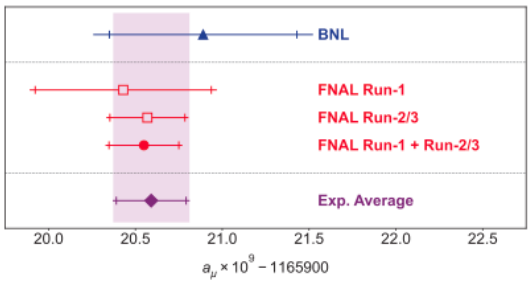

Figure 1: Experimental values of a_μ (see Section 3.2 for details). Figure from [16].

Result	Value ($\times 10^{-11}$)	Ref.
a_μ^{BNL}	116 592 089(63)	[2]
$a_\mu^{\text{FNAL, Run}-1}$	116 592 040(54)	[15]
$a_\mu^{\text{FNAL, Run}-2/3}$	116 592 057(25)	[16]
$a_\mu^{\text{FNAL, Run}-1/2/3}$	116 592 055(24)	[16]
$a_\mu^{\text{Exp. Average}}$	116 592 059(22)	[16]

Table 2: Experimental values of a_μ (see Section 3.2 for details).

4. Comparison between Theoretical and Experimental Results and Future Outlook

At present, a firm comparison between the theoretical and experimental results cannot be established due to the discrepant evaluations of the LO-HVP contribution (see Section 2.3.1). This term is under scrutiny, and to clarify the situation, new computational efforts are underway to provide new lattice-QCD calculations, new e^+e^- cross-section measurements are in progress, and a new independent method, the MUonE experiment at CERN, is under development [5].

5. Conclusion

The muon anomaly (a_μ) measured using the Run-1 and Run-2/3 data from the Fermilab Muon g-2 experiment confirms the previous result from the BNL experiment, improving the world average uncertainty to 190 ppb. Comparison of this measurement with the Standard Model prediction could point to new physics, but currently, the uncertainty of the theoretical calculation is limited by the evaluation of the hadronic contributions. While efforts are in progress to clarify the theoretical situation, the Fermilab Muon g-2 Collaboration is analyzing the Run-4/5/6 data, which are expected to reduce the uncertainty of the muon anomaly experimental measurement to 140 ppb.

Acknowledgments

This work was supported in part by the US DOE, Fermilab, the Istituto Nazionale di Fisica Nucleare (Italy), and European Union STRONG 2020 project under grant agreement No. 824093.

References

[1] P. Dirac, "The Quantum theory of electron. 2.," Proc. Roy. Soc. Lond. A **118**, 351 (1928).

[2] G. W. Bennett *et al.* [Muon g-2], "Final Report of the Muon E821 Anomalous Magnetic Moment Measurement at BNL," Phys. Rev. D **73**, 072003 (2006).

[3] T. Aoyama, N. Asmussen, M. Benayoun, J. Bijnens, T. Blum, M. Bruno, I. Caprini, C. M. Carloni Calame, M. Cè and G. Colangelo, *et al.* "The anomalous magnetic moment of the muon in the Standard Model," Phys. Rept. **887**, 1-166 (2020).

[4] S. Borsanyi, Z. Fodor, J. N. Guenther, C. Hoelbling, S. D. Katz, L. Lellouch, T. Lippert, K. Miura, L. Parato and K. K. Szabo, *et al.* "Leading hadronic contribution to the muon magnetic moment from lattice QCD," Nature **593**, no.7857, 51-55 (2021).

[5] The Status of Muon g-2 Theory in the Standard Model, 2023. URL: https://muon-gm2-theory.illinois.edu, statement updated on August 10, 2023 in view of the announcement of the second result by the Muon g-2 experiment at Fermilab.

[6] F. V. Ignatov *et al.* [CMD-3], "Measurement of the $e^+e^- \to \pi^+\pi^-$ cross section from threshold to 1.2 GeV with the CMD-3 detector," Phys. Rev. D **109**, no.11, 112002 (2024)

[7] G. Colangelo, M. Davier, A. X. El-Khadra, M. Hoferichter, C. Lehner, L. Lellouch, T. Mibe, B. L. Roberts, T. Teubner and H. Wittig, *et al.* "Prospects for precise predictions of a_μ in the Standard Model," [arXiv:2203.15810 [hep-ph]], (2022).

[8] J. Grange *et al.* [Muon g-2], "Muon (g-2) Technical Design Report," [arXiv:1501.06858 [physics.ins-det]], (2015).

[9] D. Stratakis, B. Drendel, J. P. Morgan, M. J. Syphers and N. S. Froemming, "Commissioning and First Results of the Fermilab Muon Campus," Phys. Rev. Accel. Beams **22**, no.1, 011001 (2019).

[10] T. Albahri *et al.* [Muon g-2],"Magnetic-field measurement and analysis for the Muon g-2 Experiment at Fermilab," Phys. Rev. A **103**, no.4, 042208 (2021).

[11] T. Albahri *et al.* [Muon g-2], "Measurement of the anomalous precession frequency of the muon in the Fermilab Muon g-2 Experiment," Phys. Rev. D **103**, no.7, 072002 (2021).

[12] $\mathcal{F}_{ext}$ is equal to the product of the following four terms:
- $\mu'_p(Tr)/\mu_e(H)$, the ratio of the magnetic moment of the proton in a spherical water sample at 34.7 °C and the magnetic moment of the electron in a hydrogen atom;
- $\mu_e(H)/\mu_e$, the ratio of the magnetic moment of the electron in a hydrogen atom and the magnetic moment of the free electron in vacuum;
- m_μ/m_e, the ratio of the muon and electron masses;
- $g_e/2$, the electron gyromagnetic factor divided by 2.

[13] D. P. Aguillard *et al.* [Muon g-2], "Detailed report on the measurement of the positive muon anomalous magnetic moment to 0.20 ppm," Phys. Rev. D **110**, no.3, 032009 (2024).

[14] T. Albahri *et al.* [Muon g-2], "Beam dynamics corrections to the Run-1 measurement of the muon anomalous magnetic moment at Fermilab," Phys. Rev. Accel. Beams **24**, no.4, 044002 (2021).

[15] B. Abi *et al.* [Muon g-2], "Measurement of the Positive Muon Anomalous Magnetic Moment to 0.46 ppm," Phys. Rev. Lett. **126**, no.14, 141801 (2021).

[16] D. P. Aguillard *et al.* [Muon g-2], "Measurement of the Positive Muon Anomalous Magnetic Moment to 0.20 ppm," Phys. Rev. Lett. **131**, no.16, 161802 (2023).